

OPTICAL NAVIGATION FOR DAWN AT VESTA⁺

Nickolaos Mastrodemos*, Brian Rush*, Drew Vaughan*, Bill Owen*

The Dawn S/C, launched in September 2007, towards Vesta and Ceres, will enter into orbit about asteroid Vesta in July 2011 and will conduct science remote sensing operations for approximately one year at various orbital altitudes. Vesta navigation operations begin with early approach in May 2011 until departure to Ceres in July 2012. A key navigation aspect is optical navigation, which will be conducted at all mission phases. Here we review the optical navigation plan, imaging, methodology, data types, as well as expected performance in the context of the overall mission navigation. A key aspect of optical navigation at Dawn that will receive particular attention is the extensive use of landmark navigation during most of mission phases. In addition to supporting real-time navigation operations, optical navigation will be used to determine some key physical characteristics of Vesta, such as the asteroid's pole & shape, to assist mission design & science operations.

MISSION OVERVIEW

After more than 3 1/2 years of interplanetary cruise the Dawn S/C will begin its final approach towards asteroid Vesta in May 2011. According to the current mission plan approach operations will commence on May 3, with orbit capture on July 14, entry to the first science orbit on August 8 and will be concluded in July 2012. Vesta operations are roughly divided into 2 distinct types; approach and orbit transfers and the science orbits. During approach and orbit transfers the S/C is in near-continuous low-thrust mode with the Ion Propulsion System, with short coasting periods for collecting tracking & optical data as well as engineering telemetry. During the science orbits, where the bulk of the science observations are collected, the S/C is coasting in near polar orbits about Vesta.

The scientific investigations are based on remote sensing observations conducted by the Framing Camera (FC), the Visual & Infrared Recorder (VIR) and the Gamma Ray and Neutron Detector (GraND). In addition radiometric tracking data are collected for the gravity investigation. During each of the science phases a particular instrument is prime, determining most of the data collection strategy and pointing at that particular phase.

A breakdown of mission phases in chronological order, current time allocation, and key goals and observations are as follows;

Approach phase: It begins ~100* days prior to orbit insertion. It is mostly a navigation phase during which the range to Vesta decreases from 160,000 km to 3000 km and the S/C is first

+ © 2011 California Institute of Technology. Government sponsorship acknowledged

* Optical Navigation Group, Sec343, Jet Propulsion Laboratory, California Institute of Technology, Pasadena, CA, 91109

gravitationally captured and then spirals towards a polar orbit. The main scientific investigations are the determination of Vesta's pole vector, the phase function and the search for satellites and orbital debris

Survey: It has a duration of 6 orbits, or ~16 days, at a targeted radius of 3000 km, inclination 90°, and a beta angle, defined as the angle between the orbit plane and the Sun, of 15°. The prime instrument is VIR for the surface spectral & mineral composition. In addition a number of FC mosaics as well as observations of opportunity will be acquired that will allow for a global topographic coverage of the body. For a polar orbit the beta angle is also the minimum phase angle at the equator. Orbital period is ~68 hours.

High Altitude Mapping Orbit 1 (HAMO-1): Duration of 62 orbits, or ~29 days for a targeted radius of 900 km. Beta angle is 30°. The key science investigation is the Vesta surface topographic reconstruction with the FC being the primary instrument. This phase is broken into 6 imaging cycles. Each cycle consists of 10 orbits that allow complete surface coverage at a particular pointing direction relative to Vesta center. Cycles #1 and #6 are nadir, and the remaining 4 are at fixed off-nadir direction each. The orbital period is ~11.2 hours.

Low Altitude Mapping Orbit (LAMO): The duration of this phase is 8-10 weeks at a radius of 450 km and beta angle 45°. The orbit period is 4 hours. The primary instrument is GRAND. Main science goals are the mineral and elemental abundances. Another key investigation is that of the gravity field for which tracking data will be acquired. The pointing is strictly nadir. FC and VIR nadir observations of opportunity are also acquired.

High Altitude Mapping Orbit 2 (HAMO-2): This is the last science orbit. It is a repeat of **HAMO-1**, at the same radius but higher beta angle, 45° that will allow surface mapping of the north latitudes, > 47°, which are not visible in **HAMO-1**. It is divided in 4 cycles, with 1 cycle being nadir imaging and the other three cycles off-nadir.

Transfers: These are periods of almost-continuous thrusting with the interruption for acquisition of navigation data. During these periods the S/C spirals between science orbits. The approximate duration of the transfers is Survey-to-HAMO-1 28 days, HAMO-1-to-LAMO 39 days and LAMO-to-HAMO-2 42 days.

NAVIGATION PAYLOAD

Images for OpNav will be furnished by the Framing Cameras, built and operated by the Max-Planck Institute for Solar System Research at Lindau (MPS). For redundancy there are two, identically built cameras, referred to as FC1 & FC2. Even though their main scientific objective is surface mapping, their astrometric properties are sufficient for navigation. One of these, FC2, is the primary camera during operations, with FC1 being the secondary one in case of an anomalous behavior of FC2. The cameras, as well as the rest of the payload, are nominally co-aligned, with the boresight along the S/C +Z axis. The detector is a standard frame transfer CCD with the sample direction along the S/C X-axis and the line direction along the S/C Y-axis.

Some relevant parameters of the camera are described below

- Aperture size 19 mm
- Refractive optics
- Focal length nominal 150 mm
- Pixel size 14 μm
- FOV 5.5°x 5.5°, IFOV 93.3 μrad
- 1024 x 1024 frame transfer CCD

- 14-bit digitization
- both lossless and lossy compression
- approximately 1 DN readout noise

Both cameras have been operated and tested in flight. Tests include photometric calibration, with both standard stars such as Vega and solar analogs, point-spread function measurements, geometric calibration for measuring the focal length and distortion parameters using open cluster NGC3532. Based on these in-flight measurements the clear filter response between FC2 and FC1 differ by less than 5%. The current prediction is that for a 1 sec exposure at zero phase the mean brightness of an extended Vesta is $\sim 1.1 \times 10^6$ DN per pixel. The stellar point-spread function is quite narrow, measured at ~ 1.2 pixels FWHM, still adequate for astrometric observations.

The cluster observations were used to derive a 6 parameter distortion model that includes the focal length, the ratio of pixel scale in the sample and line direction, (departure from square pixels), the deviation from rectangular pixels, cubic distortion as well as tilts of the focal plane along the sample and line direction. The post-fit residuals of the calibration data to this distortion model are for both cameras ~ 0.09 pixel $1-\sigma$. When imaging a few stars, 5-10, with signal-to-noise (SNR) > 10 , the camera's inertial pointing is estimated to a post-fit RMS of 0.09 - 0.11 pixels, which is more than adequate for navigation at Vesta.

The alignment of the cameras to the S/C frame was measured using the cluster observations to establish the camera's inertial pointing, that we considered to be the "truth" due to their much higher accuracy and comparing it to the camera's pointing as deduced from the reconstructed attitude telemetry, provided by the Attitude Control System (ACS) which describes the mean attitude knowledge. The alignment was measured by computing 3 Euler angles, or equivalently the 3x3 rotation matrix that describe the rotation between the camera and S/C frames. The misalignment of FC2 compared to its nominal mounting amounts to 37 pixels perpendicular to the boresight and 0.08° about the boresight. The corresponding figures for FC1 are 12.5 pixels and 0.06° . The post-fit RMS accuracy of these alignments is ~ 0.4 pixel ($1-\sigma$) when projected perpendicular to the focal plane. When the camera to S/C alignment is accounted for, the residual pointing error between the camera pointing from the reconstructed attitude telemetry and that from the stars is found to be in the 1-2 FC pixels range and mostly random. Any misalignment represents a fixed attitude bias, which can have important implications for navigation accuracy. When we acquire Vesta observations without any stars present, the camera pointing is provided from the reconstructed ACS attitude. Since the camera pointing solution correlates with the S/C Vesta position vector a pointing bias will affect the S/C-Vesta relative state estimation. Ideally we want to be left with only a random pointing ACS error.

The scattered light properties of FC2, including any stray-light from mechanical structures, were measured by imaging stars while positioning the camera's boresight at specific angles relative to the sun, in the range of $90^\circ - 20^\circ$ and at 2.5° , or $\sim 1/2$ FOV intervals. No appreciable stray-light levels were measured for sun angles $> 30^\circ$, which correspond to Vesta geocentric phase angles of 150° , a viewing condition that we do not plan to utilize. In addition the camera has an athermal design that allows minimum barrel expansion while observing at low Sun angles, $< 60^\circ$. That was verified during the lengthy stray-light test, where there was no measurable change to the focal length.

The only other important in-flight information that we lack is the in-field and out-of-field properties in the presence of a very bright object. Such data were scheduled to be acquired on Feb 10 2009, during the closest approach of the Mars flyby. However, due to a safing event, these

images were not acquired. Consequently, we currently cannot predict the effect of the bright disk of Vesta on star images, located just of the limb.

OPTICAL NAVIGATION OVERVIEW

Optical navigation will be used throughout all mission phases from early approach to the end of HAMO-2. The main tasks of OpNav are the contributions to the ongoing orbit determination efforts, for trajectory design and control, payload pointing and trajectory reconstruction. Other data types that will be used for orbit determination are DDOR early on approach, and Doppler and range throughout. Other important tasks include the estimation of Vesta's pole, especially on approach where for the most part the only contribution comes from the optical data, and the determination of Vesta's shape model for updates in the planning of the FC and VIR image acquisition.

For most aspects of OpNav planning and processing, the size of Vesta is the single most important parameter. Early approach starts with Vesta ~ 5 FC pixels and ends with Vesta $2 \times \text{FOV}$. During LAMO Vesta is $\sim 25 \times \text{FOV}$. During early approach most image planning and processing is inertial-based, up to when Vesta is ~ 500 FC pixels. Subsequently image planning is Vesta-centered. Similarly, different data types are used depending on the size of Vesta; during early approach and while Vesta is ≤ 500 - 700 FC pixels limb scans along the lit-limb of the asteroid are going to be used to estimate the center of figure^{3,4}. When Vesta exceeds ~ 50 FC pixels, landmarks will also be introduced (ref). Both data types will be used concurrently until in late approach when Vesta exceeds ~ 700 FC pixels, from which point on, landmarks will be used exclusively.

DATA PROCESSING & METHODOLOGY

Data types

The key optical data types are limb scans and landmarks. Limb scans will be used from early approach until Vesta exceeds ~ 700 FC pixels, whereas landmarks will be used from mid-approach, Vesta ~ 40 - 50 pixels, to the end of the mission. Both data types will be used during a certain time period on approach in 2 steps; 1) first limb scans will be processed to assist in a first combined S/C, asteroid state solution, 2) a new S/C and Vesta ephemeris will be constructed that will be used to construct and process the landmarks.

Limb scans. These are observations of the location of the limb of the object, in order to estimate its center of figure (COF). They have been used extensively with the Cassini & Voyager missions⁵. Scan lines are constructed, either radially based on the apriori COF or normal to the predicted limb of the body. The predicted limb location is derived from an apriori shape model, which could be either a triaxial ellipsoid or an arbitrary shape modeled by Legendre polynomials. A model brightness profile is constructed, using typically a Minnaert reflectance model and correlated with the image-extracted brightness profile to determine the location of the limb along each scan line and subsequently the COF. The number of scan lines is determined automatically based on a maximum input number and the extent of the illuminated limb. The accuracy of the method is dependent on the size of the body and the accuracy of the apriori shape. With a well-determined shape for a body in the 50-100 pixel range the $(1-\sigma)$ COF pixel, line position error is $\sim 3\%$ - 5% the apparent body radius and for larger bodies at the 1-2% of the radius. Clearly as Vesta grows in the FOV during approach the accuracy of the method flattens to a fixed centerfinding metric error. The shape models currently in use are a triaxial ellipsoid and an arbitrary shape based on Vesta HST observations⁶. The triaxial ellipsoid has axes $A=289$ km, $B=$

280 km and $C=229$ km. These models will also be used during early approach processing until an updated model will be constructed from landmarks. The above centerfinding estimates were also confirmed with OpNav processing simulations based on simulated approach Vesta images. Figure 1 shows such an example with the arbitrary shape assumptions.

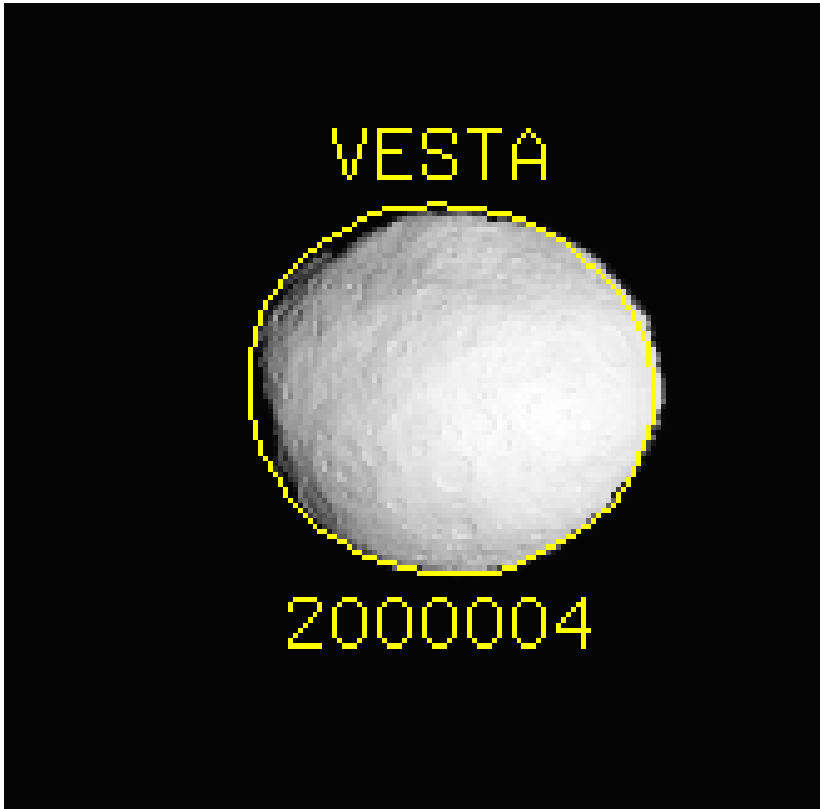


Figure 1. Simulated image of Vesta with the outline of the shape model superimposed for limb-scan processing. Image resolution is 7 km/pixel.

Landmarks. For proximity operations, especially when the body size exceeds the FOV, landmarks are more suitable data types. Landmarks have been used in the past for navigating about asteroid Eros⁷. With NEAR, landmarks were identified with specific body features, most commonly crater rims. Their identification and image registration required a number of image pixels with the attendant loss of astrometric accuracy. Here we use a more generalized version; landmarks are control points, fixed in the body frame, that are at the center of small digital terrain and albedo model, or landmark map (L-map), that extends over a small part of the total surface. They are not linked to specific surface features, in fact no distinct features are needed; their identification and construction via an L-map requires only a modest brightness contrast of 3-4. L-maps are constructed with stereo-photoclinometry (SPC) the formulation of which has been presented elsewhere^{8,9,10}.

The association of a landmark with an L-map brings about many new advantages some of which are;

- a) the 3-d properties of the L-map allow use of a large number of images at varying resolutions, incidence and emission angles; 0° - 60° or even larger emission and up to 80° in incidence, image resolutions varying by a factor up to 20 (we typically use ~ 10) and number of images from a minimum of 3 to hundreds.
- b) Cross-correlation techniques are used to register images on the surface and neighboring L-maps overlapping the same surface element with each other, to a much higher center-finding accuracy, < 0.1 pixel.
- c) Identification of L-maps in illuminated limbs of images and association of L-maps with nearby ones that share common topography increases the constraints applied for global solutions that estimate S/C position, camera pointing and landmark location.
- d) A systematic tiling of the surface with can be performed, at prescribed landmarks spacing that again allows for a more self-consistent global solution
- e) Automatic search and identification of existing landmarks in new images allows for quick navigation turnaround
- f) Synthesizing the L-maps into a global topography model improves the surface registration of new images.

Key Processing steps for a single L-map

The main steps in the construction of L-maps are as follows;

- a) The approximate location of the map center is specified, usually based on an image coordinate location or on latitude and longitude. The map pixel scale and size, typically 99×99 pixels, is also specified. A schematic of the local map geometry is shown in Fig. 2; all relevant vectors are rotated to a body-fixed reference frame, including the camera vectors, \mathbf{c}_i ($i=x,y,z$) and the local L-map local coordinate system \mathbf{u}_i , ($i=x,y,z$)
- b) Based on apriori camera pointing, S/C trajectory and shape model all images that overlap with the map are queried and those found suitable based on certain geometric criteria are retained. Criteria include the incidence and emission angle, usually in the range of 0° - 60° , and 10° - 80° respectively, although if sufficient images are available the preferred incidence angles are $> 30^{\circ}$. The criteria also include the L-map to image resolution with the preferred values in the $3 - 1/3$ range.
- c) Image templates that overlap the L-map are resampled to the map pixels and normally projected on the map based on the apriori topography (ortho-rectified).

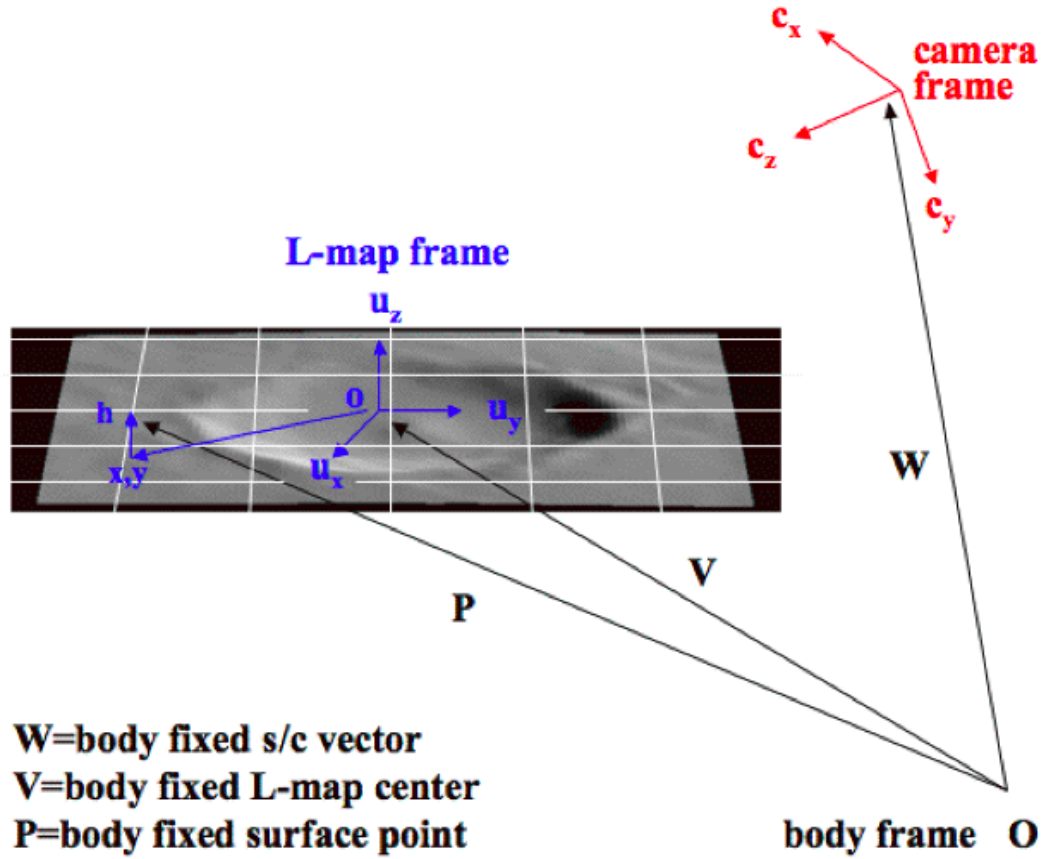


Figure 2. landmark geometry

- d) At each map pixel \mathbf{x} , a predicted brightness model is constructed for each projected image,

$$I_k(\mathbf{x}) = \Lambda_k(1+a(\mathbf{x})) R(i,e) + \Phi_k, \quad (1)$$

where a is a relative albedo parameter, normalized so that over each L-map has a zero mean, $R(i,e)$ is the reflectance function, i and e , the incidence and emission angles and Λ_k, Φ_k parameters specified on per image basis. If $\mathbf{t}=(t_1,t_2)$ are the slopes on each L-map pixel, the photometric model is related to the slopes and local geometry by the relations,

$$\cos i = (s_3-s_1t_1-s_2t_2)/\sqrt{(1+t_1^2+t_2^2)}, \quad \cos e = (c_3-c_1t_1-c_2t_2)/\sqrt{(1+t_1^2+t_2^2)} \quad (2)$$

where \mathbf{c} is the camera unit vector and \mathbf{s} the body-sun unit vector.

The reflectance function could include phase parameters as well. In its simplest form it is a linear combination of a Lambert and Lommel-Seeliger law. Due to the small spatial extent of the L-map, the photometric fit to the data is not sensitive to an accurate phase function. For Vesta such phase effects may bear some significance during late approach & Survey where each image is within a factor of two of the FOV so that there could be phase effects across the size of the map. To the extent possible we plan to replace our simple reflectance function

with one based on a Hapke model if such parameters can be extracted from the approach images¹¹.

- e) At each map pixel the albedo and slopes are estimated by performing a least squares fit between the extracted brightness template from each image and the predicted one based on the above brightness model. Because at this stage the image templates are extracted based on apriori position and pointing information they are not necessarily aligned with each other. As a result the model image brightness appears fuzzy. The model image brightness is re-illuminated at the nominal image geometry, cross-correlated with each image template, which is shifted based on the peak in the correlation measure. The process is repeated until a correlation maximum is reached and the image template shifts have converged.
- f) The heights are determined via a relaxation process from the slopes and the nearest neighbor heights. The process requires certain initial seed heights, which are stochastically sampled, from the existing shape model, nearby L-maps or limb points. This process is repeated many times until convergence is reached.
- g) The final step in the L-map construction is to search for the limb points and nearby map L-map overlaps which are important constraints in the global data fit. Images for which the L-map can be located on part of their illuminated limb are identified and the image coordinate near the limb of the corresponding landmark is recorded. The limb condition provides an additional constraint to the camera pointing in the direction perpendicular to the limb, as well as height constraints in the L-map. For nearby maps that share common topography with the current L-map cross-correlation in the overlap area provides an independently derived relative position between the corresponding landmark vectors, which in principle will differ from the ones determined at step e) above. This relative vector constitutes an additional input for the global landmark solution.

Global geometry solution

The process described above is repeated to tile systematically all available surface area covered by the current images. At this point the landmark vectors are known only approximately, because their position on the surface depends on the current topography knowledge and the *a priori* S/C-Vesta position and camera pointing. The next step is to solve for the landmarks, S/C-Vesta position and camera pointing. A global weighted least-squares estimate is performed that minimizes the sum square residuals between the predicted and observed landmark image positions. The relevant weights are chosen to reflect the current knowledge of the uncertainty of the contributing terms. The process is iterative with first solving for the landmark vectors, then for the S/C-Vesta position and camera pointing. Finally when this step has converged other quantities such as the pole vector can be estimated. The constraints that enter in each parameter estimation are as follows;

Landmarks; 1) a height constraint from the apriori height model, aimed at keeping the landmark vector from diverging early in the iteration. 2) The relative landmark positions from the neighboring overlapping L-maps, 3) The nominal S/C position and camera pointing values 4) Limb points for landmarks identified at image limbs.

Relative position and camera pointing; 1) The nominal S/C position and pointing, 2) the landmark vector location in image space 3) limb point locations in L-maps, 4) image-to-image position correlation, so that images adjacent in time do not suffer from a random point-to-point position correction.

It should be noted that the estimation of the S/C state is limited in scope to only position and also it is a semi-kinematic solution using at most a few images, while neglecting the dynamical data such as Doppler, small forces, Solar radiation pressure etc. It is nevertheless important to be performed as an intermediate step within OpNav, because position is correlated with pointing and therefore cannot be ignored. In practice, the least squares fit is conditioned with somewhat tighter position apriori covariance so as not allow the solution to diverge, Following this step internal to OpNav processing, the landmarks are used in the navigation filter, together with the radiometric measurements. The inputs consist of the pixel, line landmark image coordinate, the landmark vector in Cartesian body-fixed coordinates, the diagonal elements of the landmark vector 3x3 covariance as well as image pixel & line landmark centerfinding uncertainties.

Landmark operational specifics

The particular method of landmark construction with SPC together with the timeline at various mission phases dictates a certain operational modes during proximity operations

Hierarchical landmark construction. Networks of landmarks are being constructed starting with coarse L-maps on approach and progressively increasing their resolution to follow the increase in image resolution; the first, coarse, L-maps tie the whole surface together and construct a sparse set of landmarks; subsequently higher resolution images are registered on the surface defined by the coarse maps; a higher resolution set of landmarks is constructed with the coarse topography providing the apriori height seeds for the higher resolution L-maps, which allow for more accurate landmark determination.

In this sense each mission phase feeds its topography into the next one and also creates the set of landmarks with which to navigate in the next phase; during late approach a network of landmarks of ~800 m map resolution will be constructed to assist in early survey navigation. At the end of survey a denser set of landmarks in the 150-120 m resolution will be constructed, that will be used for HAMO navigation

Multiple iterations within each data set. The image collection strategy and the need for continuous orbit determination requires revisiting each data set a number of times. This can be broken down into four distinct modes of processing, which also occur at decreasing frequency during operations;

- a) Aligning of new images; this is the first step when new images become available. Images are cross-correlated to existing L-maps and the correct landmark position in the new images is extracted. This step creates new observations that can quickly be used in the navigation filter and constitutes the most frequent form of OpNav inputs to the navigation filter. In this mode we assume that the landmarks are the “truth” and we only solve for the S/C position and camera pointing. This will be the case for most of HAMO-1 and LAMO. During these phases the data acquisition is such that only towards the end of each phase we will have a sufficient number of images, 4-5, for each surface element to compute higher resolution L-maps. Instead, the landmarks of the previous phase are going to be used for most of HAMO-1, LAMO and HAMO-2. In this regard an important difference between HAMO-1 and HAMO-2 is that for HAMO-2 the landmarks will be based on higher resolution maps, ~ 50 m/pixel, constructed with HAMO-1 observations, whereas for HAMO-1 the landmarks will be based on lower resolution maps, ~120-150 m/pixel constructed from the Survey observations.

- b) Adding the new images to the existing L-maps; this is the second processing step. L-maps are recomputed with the addition of new images, which enhances the map resolution and its overall height accuracy by the inclusion of the higher-resolution images. This step is followed by a global geometry solution and another input to the navigation filter
- c) Constructing new landmarks; as images accumulate that cover either new parts of Vesta or parts already imaged, but under better illumination and view conditions, new landmarks will be created to fill in all available parts of the terrain. We expect this process to take place more frequently on approach and Survey.
- d) Systematically tile all visible surface with landmarks at the resolution required to support navigation at the next mission phase. This will happen three times during Vesta operations; 1) at late approach we will tile the whole surface from 90° S - 50° N with landmarks at an L-map resolution of 800-700 m to assist in Survey navigation 2) at the end of Survey we tile all of Vesta with landmarks at a 150-120 m resolution to create the landmark network with which to navigate in HAMO-1. We expect that this process will produce ~12000 new landmarks. 3) At the end of HAMO-1 we tile all of Vesta with a new set of landmarks at 50 m resolution, using both the Survey & HAMO-1 images for LAMO navigation. This step will produce up to ~120 K landmarks. The last two landmark builds will require significant computational resources, and will be executed mostly in batch mode in a distributed computing environment.

IMAGE PLANNING DETAILS

OpNav will use only the clear filter images. These include images specifically acquired for OpNav, and images that are acquired by Science but have a dual usage by both teams. The image acquisition plan follows directly for the image processing needs and the methods to be used at each mission phase. In general the image acquisition plan has two goals; 1) acquire images for daily orbit determination support and 2) acquire images to construct landmarks that are needed for future processing,

A breakdown of the current imaging plan per mission phase is as follows;

Approach

There are 24 OpNav sessions in approach. Their duration and frequency increases with decreasing range to Vesta.

Survey - 100 to Survey - 50 days; Seven sessions once per week. Their duration is 1/2 hour because the image resolution is coarse, so that longitude coverage of the body is not of high importance.

Survey - 50 to Survey - 25 days; two sessions/week, most of 1-2 hours duration. Image resolution is in the range of 12 – 1.5 km. At the beginning of this phase we expect to be able to discern features on Vesta.

Survey - 25 to Survey insertion: two to three sessions/week of varying durations. Many of these images are depended on the local S/C-Vesta geometry and their acquisition time will vary with this geometry.

Including in these observations are 3 Rotational Characterizations opportunities (RC). These are combined OpNav/Science observations, acquired at approximate ranges to Vesta of 100 K km (RC1), 50 K km (RC2) and 5 K (RC3) km. They image Vesta for a full rotation period, ~ 5.3 hours, by simply pointing the instruments at Vesta nadir and letting the body rotate. They offer complete longitudinal surface coverage and as such have particular strength in the pole

estimation. In particular, RC3 is considered of such importance to OpNav, that a backup activity, RC3b of similar duration has been scheduled in the event of an anomaly. RC3 is centered at the first lit equator crossing, after the S/C completes it's first loop around the body towards Survey and is expected to offer a complete surface coverage from 40° N to -40° S. This single observation is expected to allow the construction of the bulk of the landmarks needed for Survey navigation. The last few OpNav sessions on approach are planned so as to allow, to the extent possible, a complete surface coverage up to ~50° and they are the lower resolution equivalent of a similar effort in survey. A description of the approach geometry with a number of the approach OpNavs is shown in figure 3.

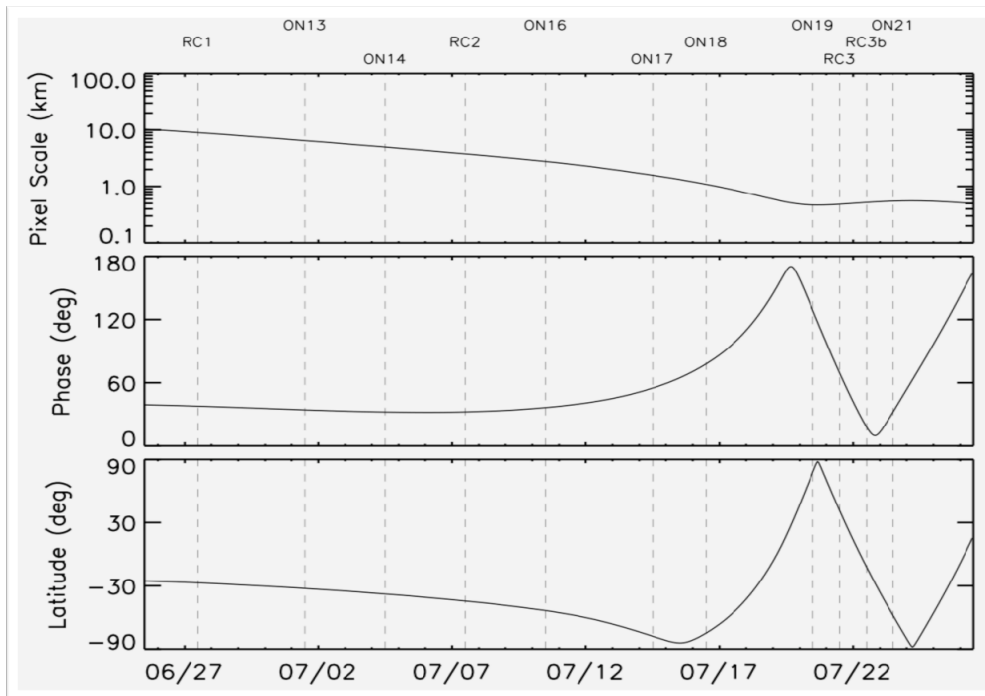


Figure 3. The viewing geometry for approach observations. Latitude denotes the sub-S/C Vesta latitude and phase is the geocentric phase angle

To the extent possible Vesta observations are also star-relative. The use of stars in the images will allow for an independent solution of the camera pointing that is to a great extent de-coupled from the estimation of other quantities, such as S/C-Vesta state, landmark vectors etc. The large brightness contrast between Vesta and the background stars prohibits simultaneous Vesta-star observations. For example for the typical phase angles on early approach, 30°-40°, we estimate that Vesta saturates the detector at ~40 ms exposures, which are too short to reveal the background stars, mostly in the 7-10 Vmag range. For that reason we acquire alternating long and short exposures, with the long exposures for stars in the 1 - 1.5 sec range and the short exposures for Vesta in the 10 – 90 ms range depending on the phase. The camera pointing is estimated from the star images as a stochastic parameter and extrapolated to the Vesta images, assuming an exponentially decaying correlation, with a typical time constant no larger than the time interval between two successive star images. Tests has shown that for a 0.1 pixel (1- σ) stochastic star image RMS post-fit residuals, the Vesta images have an accuracy of ~ 0.2 pixels, barring large

attitude motions, which is a factor of 5-10 improvement over the pointing accuracy from the ACS reconstruction. Such alternating exposures are also planned for Survey to some limited extent, but are not feasible at later mission phases.

Survey

In each survey cycle there's one 2-hour OpNav session, immediately after the dark to lit terminator crossing, of ~18 images. Each of these sessions covers a longitude band of ~80° width and a latitude range of 50° N - 20° N. All cycles put together, they provide complete longitudinal coverage of this latitude band.

Two mosaics one equatorial and one polar are acquired at certain orbits and repeated for redundancy. These mosaics extend for a full rotation period. They follow a simple 1x3 offset pattern along the line direction and aim at providing full coverage from 25° N - 90° S. In reality there are various gaps in coverage, and in practice these gaps increase due to pointing errors. A 3rd data set, which is the FC observations of opportunity, images acquired at the camera pointing driven by VIR, fill in the gaps and provide significant redundancy in the observations. All together more than 900 clear filter images are acquired in Survey, that allow landmarks to be constructed with 12 – 70 images/landmark depending on the latitude. One challenging aspect in landmark construction in Survey, is that the low beta angle results in high solar elevation, > 70°, in the equatorial band. That tends to create a mostly uniform image brightness profile with narrow, sharp features, such as crater rims providing a brightness contrast. Studies have shown that such a geometry limit the landmarks further away from the limb than would otherwise be possible, reducing the stereo coverage of the equatorial images and the height accuracy of the respective L-maps.

HAMO-1 & HAMO-2

There's no specific OpNav imaging. Instead we make use of all science clear filter observations, which are ~48/cycle for a total of ~2900 images in HAMO-1 and ~1450 in HAMO-2. For HAMO-1, two of the off-nadir cycles image Vesta at conditions that are designed to be optimal for stereo-photogrammetric methods, at similar illumination and at emission angles ~25°. The other two off-nadir cycles image Vesta at conditions that are more favorable for SPC, varying solar elevation and emission angles ~40° - 45°. Despite the large number of images the coverage at the end of HAMO-1 is such that we won't have more than 4-6 images per landmark. For navigation, therefore, we plan to use both the Survey and HAMO-1 images,

LAMO

Similarly with HAMO, there are no OpNav specific observations but a combined observational set. Imaging in LAMO is strictly nadir, with an approximate data volume of ~80 every 2 days, which is the clear image downlink frequency. Imaging in LAMO covers the surface just once, so these images are not expected to add to the topographic accuracy of the L-maps. Their use is mostly in real time navigation support.

EXPECTED PERFORMANCE

The overall setup of L-map resolution at the various mission phases & their distribution, the processing steps and the landmark navigation accuracy is studied at the highest fidelity level by simulations that are based on the latest image acquisition plan & baseline mission design.

These simulations involve the use of realistic images, including camera characteristics, S/C attitude & trajectory Vesta physical parameters, such as pole and reflectance function and their associated uncertainties. The images are processed following the same tools and processing steps as in flight operations. A great advantage of such approach is that they allow for the highest modeling fidelity. The disadvantage is that since these are not Monte-Carlo simulations, and since processing is time-consuming, only a limited range of parameter studies can be examined. The results thus extracted are used as inputs in covariance studies that explore a much larger parameter space. A summary from such simulation results showing the different sets of landmarks we will construct during Vesta operations, their resolution and respective accuracy is given in Table 1. These results will vary depending on some of the set-up assumptions, especially on the difference between the apriori and the actual surface model for Vesta, the pointing errors from ACS and the actual pole of Vesta relative to the currently assumed one.

Mission phase	Approximate number of landmarks and surface coverage	L-map pixel scale	1- σ post-fit RMS landmark-image residuals (converted to km)	1- σ post-fit RMS landmark vector uncertainty/degree of freedom
Early approach OpNav 12-18	100 90° S - 10° N	1.5 – 2 km	1.2 – 0.7	1.2 – 0.8 km
Late Approach OpNav 19-23	500 90° S - 47° N	800 m	0.4 – 0.6 km	0.5 km
End of Survey, first round	2800	300 m	90 m	140 m
End of Survey, final round	12000	120 – 150 m	90 m	80 m
End of HAMO-1	120 K	50 m	20 m	40 m

Table 1. Expected landmark characteristics and accuracy per mission phase

In Fig. 6 we show a distribution of landmarks in a Survey image between the first and the final round of their construction.

A parameter whose estimation with approach observations is important for Survey orbit entry is that of the Vesta pole. Currently the pole has an uncertainty of $> 3^\circ$ (1- σ) which needs to be reduced to $< 0.5^\circ$, prior to the last trajectory design for Survey entry. Simulations that study the reduction of the uncertainty of the pole vector with the use of landmarks have been performed. Results from such simulations can be seen in Fig. 7a,b. The pole determination may fluctuate considerably with every successive addition of OpNav images, while remaining within 1-1.5 σ of the previous formal uncertainty. Finally the addition of the RC3 global coverage images, reduce the pole uncertainty to $\sim 0.02^\circ$

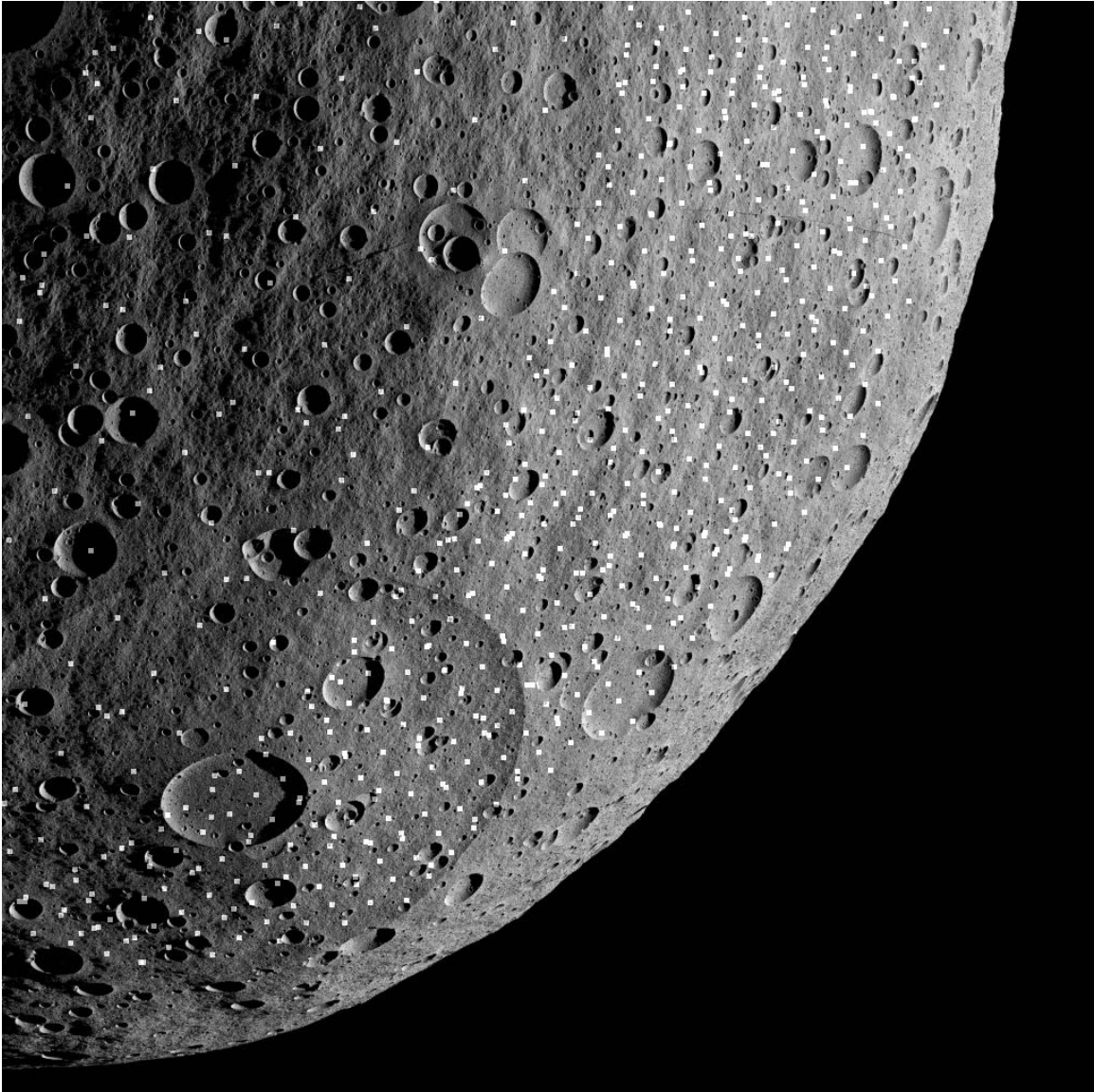
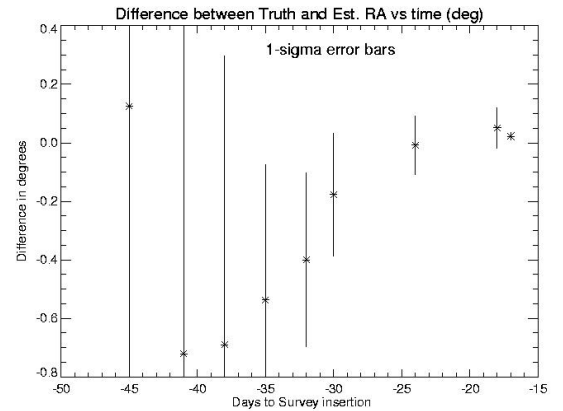
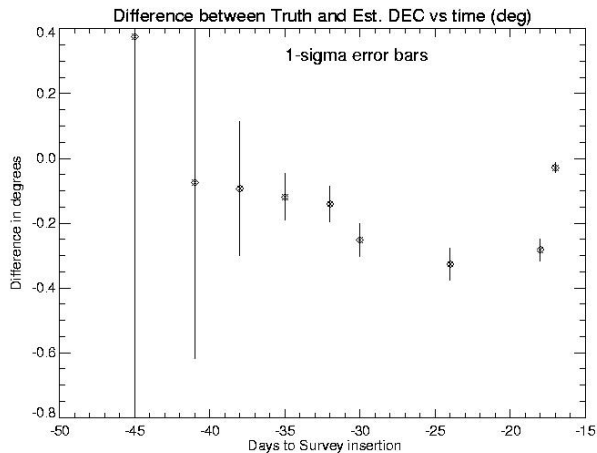


Fig 6. A simulated Survey image with the location of the landmarks marked as white squares. The more sparsely populated ones are the 800 m from late approach and the 300 m from early Survey. The densely distributed landmarks are from the systematic tiling at 150 m resolution L-maps. That tiling is still underway, so that the higher resolution L-maps have not filled the upper left of the image



Figures 7a and b, showing the reduction of the pole uncertainty as a function of days to Survey. The last data point to the right is from the RC3 data set.

ACKNOWLEDGMENTS

We are grateful to Bob Gaskell, for his continuing help and consultation on SPC as well as with his assistance with the simulated images.

This work was carried out at the Jet Propulsion Laboratory, California Institute of Technology, under a contract with NASA.

REFERENCES

⁶Thomas P.C., Binzel R.P., Gaffey M.J., Zellner B.H., Storrs A.D., Wells E., “Vesta: Spin pole, size and shape from HST images”, *Icarus* 128,, pp 88-94, 1997

³Owen W.M. Jr., Vaughan R.M. “Optical Navigation Program Mathematical Models”, Jet Propulsion Laboratory, Internal Document, 1991

⁴Owen W.M. Jr. “Methods of Optical Navigation”, AAS Paper 11-215, 21st AAS/AIAA Space Flight Mechanics Meeting, New Orleans, LA,2011

⁵Riedel J.E., Owen W.M. Jr., Stuve J.A., Synnott S.P., Vaughan R.W. “Optical Navigation During the Voyager Neptune Encounter”, AAS paper 90-2881, AAS/AIAA Astrodynamics Specialists Conference, Williamsburg, VA, 1986

⁷Owen W.M Jr., Wang T.C., Harch A., Bell M. and Peterson C. “NEAR Optical Navigation At Eros”. AAS Paper 01-376, AAS/AIAA Astrodynamics Specialists Conference, Quebec City, Canada, 2001

⁸Gaskell R.W. “Digital identification of cartographic control points”. *Photogrammetric Engineering and Remote Sensing* 54(6), Part 1, pp.723-727, 1988

⁹Gaskell, R.W. “Automated landmark identification for spacecraft navigation”. AAS paper 01-422, AAS/AIAA Astrodynamics Specialists Conf., Quebec City, Canada, 2001

¹⁰ Gaskell R.W., Barnuin-Jha O.S., Scheeres D.J., Konopliv A.S., Mukai T., Abe S., Saito J., Ishiguro M., Kubota T., Hashimoto T., Kawaguchi J., Yoshikawa K., Kominato T., Hirata N., Demura H. "Characterizing and navigating small bodies with imaging data". *Meteoritics & Planetary Science* 43, Nr 6, 1049-1061, 2008

¹¹ Hapke B. "Bidirectional reflectance spectroscopy, I. Theory". *Journal of Geophysical Research* 86: pp. 3039-3054, 1981